

Brightfield and Fluorescence Imaging Using 3D PrimeSurface Ultra-Low Attachment Microplates



Authors

Brad Larson
Agilent Technologies, Inc.
Winooski, VT, USA

Anju Dang
S-BIO
Hudson, NH, USA

Abstract

Three-dimensional (3D) cell culture has become a well established *in vitro* experimental approach as it provides an improved *in vivo*-like environment. The use of clear U bottom ultra-low attachment microplates that minimize cell adherence has become a standard for applications such as spheroid proliferation. Results shown in this application note demonstrate the ability to generate quality results using both brightfield and fluorescence microscopy.

Introduction

Culturing cells in three-dimensions (3D) has become a well established approach as it is more representative of the *in vivo* environment than traditional two-dimensional (2D) cultures. Allowing cells to interact with each other in a spheroid creates a microenvironment which mimics *in vivo* tissue and is a better model for examining the effect of drugs in cancer. Developing uniform spheroids becomes especially important as it forms the basis for robust and reliable assays. S-BIO PrimeSurface cultureware are ultra-low attachment (ULA) dishes and plates that promote scaffold-free, self-assembly spheroid formation. The plates are precoated with a proprietary hydrophilic polymer that enables spontaneous spheroid formation of uniform size. PrimeSurface 96 and 384 ULA plates have good optical clarity making them highly suitable for brightfield and fluorescent imaging. Imaging technologies such as the Agilent BioTek Cytation 5 cell imaging multimode reader allows researchers to study not only spheroid proliferation through brightfield imaging, but also phenotypic events such as hypoxia, apoptosis, or necrosis induction through the use of fluorescent probes and fluorescence imaging. Incorporation of z-stacking and projection techniques in the Agilent BioTek Gen5 microplate reader and imager software create in-focus images of spheroidal cells, allowing accurate, robust, and repeatable determination of the effect of test molecules or conditions. This application note presents data generated with Cytation 5 using PrimeSurface ULA plates to develop simple robust spheroid assays for brightfield and fluorescence imaging.

Materials and methods

Materials

Cells and media

HT-1080 fibrosarcoma cells (part number CCL-121) were purchased from ATCC (Manassas, VA). Advanced DMEM (part number 12491-015), fetal bovine serum, (part number 10437-036), and penicillin-streptomycin-glutamine (100X) (part number 10378-016) were purchased from Thermo Fisher Scientific (Waltham, MA).

Experimental components

The known topoisomerase I inhibitor, camptothecin (part number 208925) was purchased from EMD Millipore (Billerica, MA). CellTox Green Cytotoxicity Assay (part number G8731) was purchased from Promega Corporation (Madison, WI). PrimeSurface 96 U-bottom, clear-wall ULA plates (part number MS-9096UZ) and PrimeSurface 384 U-bottom, clear-wall ULA plates (part number MS-9384UZ) were donated by S-BIO (Hudson, NH).

Agilent BioTek Cytation 5 cell imaging multimode reader

The Cytation 5 cell imaging multimode reader is a modular multimode microplate reader combined with an automated digital microscope. Filter- and monochromator-based microplate reading are available, and the microscopy module provides up to 60x magnification in fluorescence, brightfield, color brightfield, and phase contrast. The instrument can perform fluorescence imaging in up to four channels in a single step. With special emphasis on live cell assays, Cytation 5 features shaking, temperature control to 65 °C, CO₂/O₂ gas control, and dual injectors for kinetic assays, and is controlled by integrated Gen5 microplate reader and imager software, which also automates image capture, processing, and analysis. The instrument was used to image spheroids in the PrimeSurface plates using brightfield and fluorescence imaging.

Methods

3D spheroid formation

HT-1080 cells were added to wells of the 96- and 384-well PrimeSurface U-bottom microplates at concentrations of 10,000, 5,000, 2,000, 1,000, 500, 250, 100, and 50 cells per well in volumes of 100 or 50 µL for the 96- or 384-well plates, respectively. The microplates were incubated at 37 °C/5% CO₂ for 48 hours to allow the cells to aggregate into spheroids.

Camptothecin treatment and dead cell staining

Upon completion of the aggregation process, a subset of spheroids seeded at 1,000 cells/well were treated with either 10,000, 500, 10, or 0 nM camptothecin by manually removing media and replacing with an equal volume of fresh media containing the drug. The plates were then incubated at 37 °C/5% CO₂ for an additional 24 hours to induce necrosis within the treated spheroidal cells. The following day, media were again removed from the wells and replaced with media containing 1x CellTox Green necrotic cell stain. The plates were incubated at 37 °C/5% CO₂ for five hours to allow fluorescent probe penetration into the cells. A final media exchange was performed to remove excess stain.

Automated imaging procedure

Spheroid imaging was carried out to assess the ability to generate quality images and accurate cellular analysis. Brightfield and fluorescent images were captured using the imaging channels listed in Table 1.

Table 1. Cell imaged per imaging channel.

Imaging Channel Target	
Brightfield	Total spheroids
GFP	Spheroidal dead cell nuclei

As the cells within the spheroids exist within a range of z-planes, a z-stacking imaging procedure was setup within Gen5. Following auto focusing, multiple images were captured above and below the focal plane to ensure that cells were imaged at the proper z-height (Table 2).

Table 2. Image z-stacking parameters.

3D Image Z-Stacking Parameters	
Focus Method	Autofocus
Number of Slices	9
Step Size	54.4 μm
Images Below Focus Point	4

3D image processing

Following capture, a z-projection of the images in the z-stack was carried out using the focus stacking algorithm to create a final image containing only the most in-focus information (Table 3).

Table 3. 3D z-projection criteria.

3D Image Stitching Parameters	
Method	Focus stacking
Channel	Brightfield
Size of Maximum Filter	11 pixels
Top Slice	9
Bottom Slice	1

Cellular analysis of 3D projected images

Cellular analysis was carried out on the projected images of untreated variable sized spheroids using the criteria in Table 4.

Table 4. Spheroid identification criteria.

Spheroid Cellular Analysis Criteria	
Channel	ZProj[Brightfield]
Threshold	10,000
Background	Light
Split Touching Objects	Unchecked
Fill Holes in Masks	Checked
Minimum Object Size	75 μm
Maximum Object Size	1,000 μm
Include Primary Edge Objects	Unchecked
Analyze Entire Image	Checked
Advanced Detection Options	
Rolling Ball Diameter	Auto
Image Smoothing Strength	0
Evaluate Background On	5% of lowest pixels
Analysis Metric	
Metric of Interest	Spheroid volume

An additional cellular analysis step was performed on the treated spheroids to determine the extent of necrotic activity induced by the camptothecin treatment (Table 5).

Table 5. Spheroid necrosis induction analysis criteria.

Spheroid Necrosis Induction Analysis Criteria	
Primary Mask Criteria	
Channel	ZProj[Brightfield]
Threshold	25,000
Background	Light
Split Touching Objects	Unchecked
Fill Holes in Masks	Checked
Minimum Object Size	200 μm
Maximum Object Size	1,000 μm
Include Primary Edge Objects	Unchecked
Analyze Entire Image	Checked
Advanced Detection Options	
Rolling Ball Diameter	600
Image Smoothing Strength	0
Evaluate Background On	5% of lowest pixels
Secondary Mask Criteria	
Channel	ZProj[GFP]
Measure Within a Secondary Mask	Checked
Expand Primary Mask	1 μm
Threshold	30,000
Smooth	0
Method	Threshold in mask
Fill Holes in Mask	Unchecked
Analysis Metric	
Metric of Interest	Object area
Metric of Interest	Area_2[ZProj[GFP]]
Custom Metric of Interest	% Necrotic cell area

Results and discussion

Brightfield imaging of formed spheroids

Visual analysis of the z-projected images reveals that HT-1080 cells are able to form tight spheroids within the 96-well U-bottom plates. It is also evident that the z-stacking and projection method used by the Gen5 microplate reader and imager software creates accurate, in-focus spheroidal images regardless of size (Figure 1).

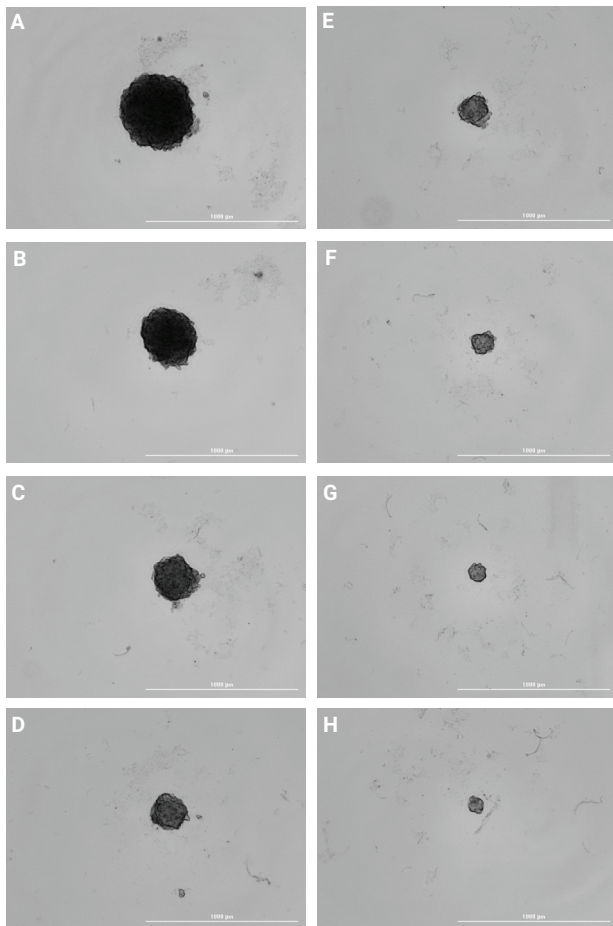


Figure 1. 96-well U-bottom brightfield spheroidal imaging. 4x z-projected brightfield images of spheroids formed from (A) 10,000; (B) 5,000; (C) 2,000; (D) 1,000; (E) 500; (F) 250; (G) 100; or (H) 50 cells per well.

A final observation apparent from the images is the flat, or even background signal generated from the bottom of the microplate wells during brightfield imaging. Using the Line Profile tool available in Gen5, a line can be drawn from one side of an image to the other, bisecting the spheroid (Figure 2A). This creates a brightfield intensity graph representative of the CCD pixel intensities along the line. It is evident that there is a large decrease in pixel intensity as the line passes through the spheroid and that the other pixels representative of background are relatively bright and uniform in intensity (Figure 2B).

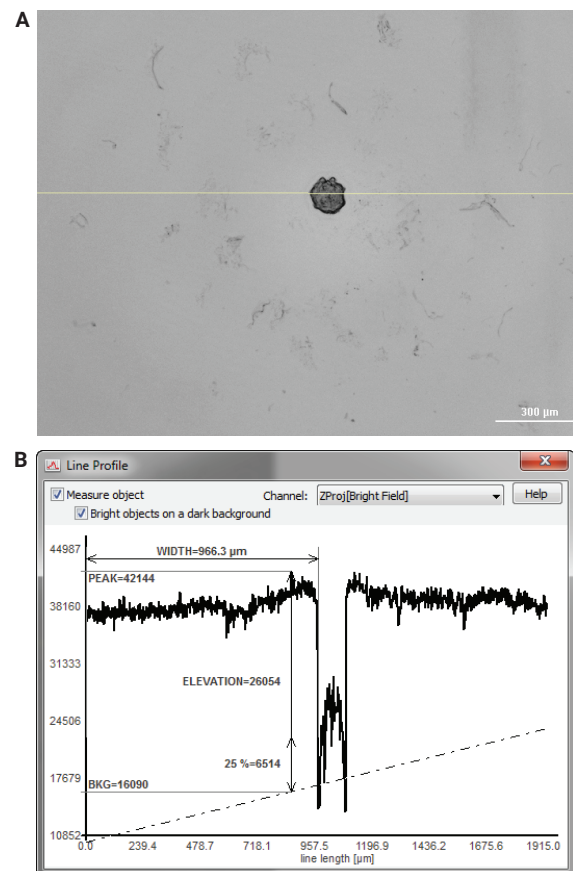


Figure 2. Image background and target object brightfield signal. (A) 4x brightfield image of a 100-cell spheroid plus a line drawn with the View Line Profile tool. (B) Graph of the brightfield signal from the 1,915 µm drawn line.

Figure 3 demonstrates the accurate placement of primary masks necessary for area and diameter measurements using parameters in Table 4. Using the two metrics, a volume calculation can be made.

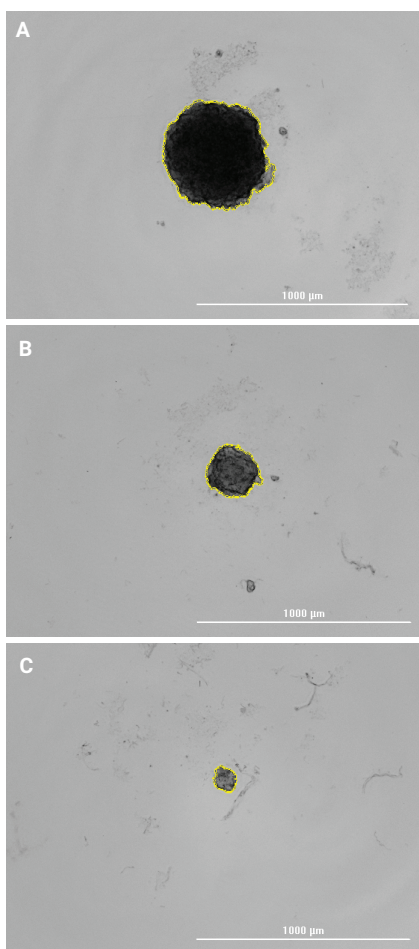


Figure 3. Cellular analysis of test spheroids. Agilent BioTek Gen5 microplate reader and imager software automatically drawn object masks around spheroids formed from (A) 10,000, (B) 1,000, and (C) 50 cells.

Spheroid analysis was performed in both 96- and 384-well PrimeSurface plates. Figure 4 illustrates the precision and linearity of spheroid volume as a function of cell seeding density.

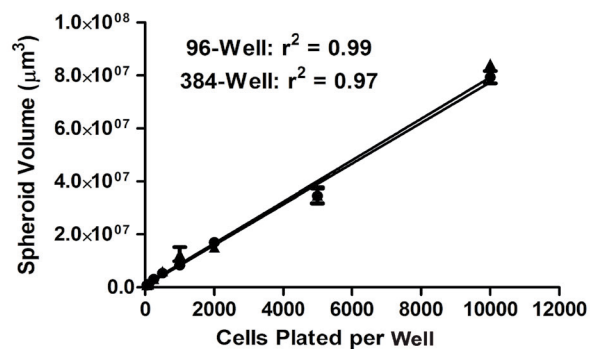


Figure 4. Plot and linear regression of Agilent BioTek Gen5 96- and 384-well calculated spheroid volumes.

Florescent imaging of necrotic cell induction within spheroids

Imaging was also carried out on treated and stained 1,000-cell spheroids to determine the level of necrotic cell induction caused by camptothecin. Brightfield images were captured, in addition to fluorescent images in the GFP channel to specifically view necrotic cells stained by the CellTox Green probe. An overlay was then created to visualize cellular necrosis within each spheroid (Figure 5A).

To quantify the level of induced necrosis, cellular analysis was once again performed on the spheroidal images. To determine the area covered by both live and dead cells within the captured images, object masks were placed around the spheroids (Figure 5B) using the brightfield channel and primary mask criteria described in Table 5.

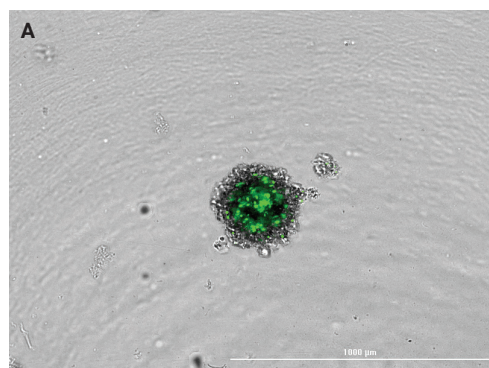


Figure 5A. Imaging of camptothecin induced spheroidal cell necrosis. 4x z-projected, overlaid brightfield, and GFP image of a spheroid showing necrotic cell induction caused by 24-hour 10,000 nM camptothecin.

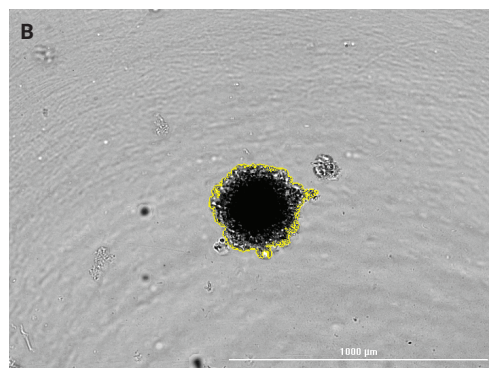


Figure 5B. Primary cellular analysis to determine necrotic cell induction. Agilent BioTek Gen5 microplate reader and imager software automatically drawn primary object masks around a 1,000-cell spheroid treated with 10,000 nM camptothecin.

The second step was to quantify the area covered solely by necrotic cells within each test spheroid. A concern, though, with using clear walled microplates to perform fluorescence imaging and then ascertain accurate results is the autofluorescence from the clear walls, contributing to high background within the image. Use of the Gen5 Line Profile tool, however, confirms that this phenomenon was not witnessed when using the clear U-bottom microplates (Figure 6A). A consistently low background signal was seen from areas of the image not containing necrotic cells, allowing for an easily distinguishable change in signal from affected cells (Figure 6B).

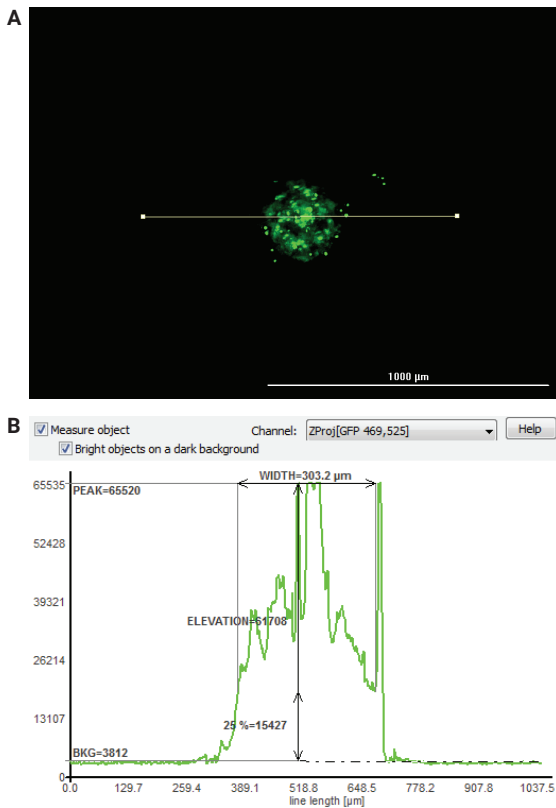


Figure 6. Image background and target object fluorescent signal. (A) 4x GFP image of a 1,000-cell spheroid treated with 10,000 nM camptothecin, plus a line drawn with the View Line Profile tool. (B) Graph of the GFP signal from the 1,037 μm drawn line.

By taking advantage of the optical qualities of the U-bottom plates, accurate object masks were able to be placed around affected cells, regardless of whether high or low levels of necrotic activity were generated by the camptothecin concentrations (Figure 7).

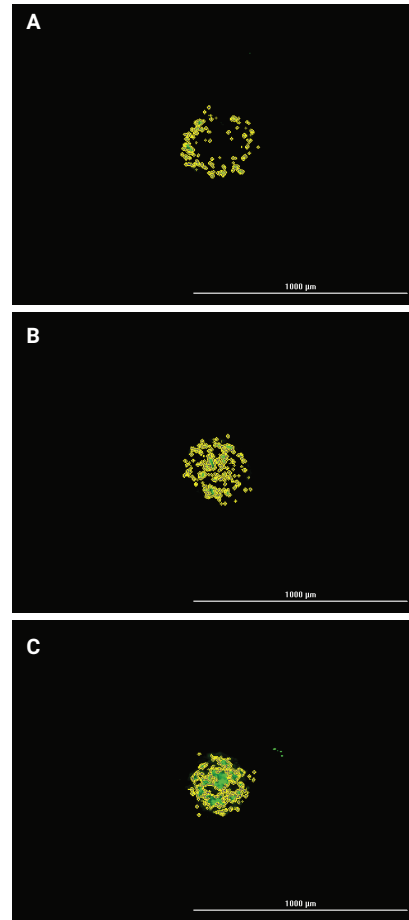


Figure 7. Necrotic cell analysis of treated spheroids. Agilent BioTek Gen5 automatically drawn object masks around necrotic cells within spheroids treated with (A) 10; (B) 500; or (C) 10,000 nM camptothecin.

When the necrotic cell area was divided by the total cell area, a normalized affected cell percent coverage area was created, which accounted for variances in area between the treated 1,000 cell spheroids. The values were then plotted in terms of the concentration of camptothecin used for treatment (Figure 8).

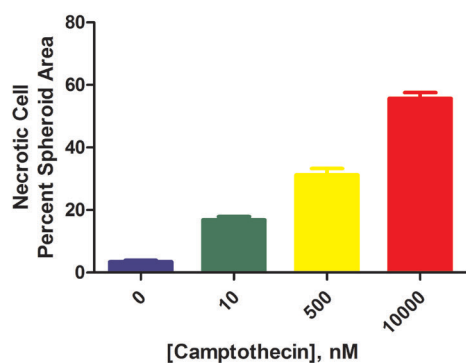


Figure 8. Plot of percent spheroid area covered by affected necrotic cells following camptothecin treatment.

The images in Figure 7 of object mask placement based upon GFP signal, in addition to the graph of camptothecin-induced spheroidal cell necrosis, confirms that accurate imaging and analysis can be carried out when using fluorescent channels and the U-bottom microplates.

Conclusion

S-BIO PrimeSurface U-bottom 96- and 384-well microplates can be used to create appropriately sized, repeatable single spheroids within each test well. The Agilent BioTek Cytation 5 cell imaging multimode reader and Agilent BioTek Gen5 microplate reader and imager software also provide the ability to capture high-quality images on multiple z-planes, suitable for spheroid imaging. The combination of the optical quality of the microplates and Gen5 software allow accurate quantification of proliferation or induced phenotypic events within the spheroids using either brightfield or fluorescence microscopy.

www.agilent.com/lifesciences/biotek

For Research Use Only. Not for use in diagnostic procedures.

RA44412.5299884259

This information is subject to change without notice.

© Agilent Technologies, Inc. 2017, 2022
Printed in the USA, March 31, 2022
5994-3389EN